

Self-Accelerating Self-Trapped Optical Beams

Ido Kaminer,¹ Mordechai Segev,¹ and Demetrios N. Christodoulides²

¹*Physics Department and Solid State Institute, Technion, Haifa 32000, Israel*

²*CREOL—College of Optics and Photonics, University of Central Florida, Orlando, Florida 32816, USA*

(Received 22 September 2010; published 26 May 2011)

We present self-accelerating self-trapped beams in nonlinear optical media, exhibiting self-focusing and self-defocusing Kerr and saturable nonlinearities, as well as a quadratic response. In Kerr and saturable media such beams are stable under self-defocusing and weak self-focusing, whereas for strong self-focusing the beams off-shoot solitons while their main lobe continues to accelerate. Self-accelerating self-trapped wave packets are universal, and can also be found in matter waves, plasma, etc.

DOI: 10.1103/PhysRevLett.106.213903

PACS numbers: 42.65.Tg

In 1979, Berry and Balazs [1] found accelerating wave functions for the potential-free Schrödinger equation. In 2007, self-accelerating optical Airy beams were demonstrated [2]. This phenomenon has drawn much interest with applications ranging from trapping particles along curved paths [3] to self-bending plasma channels [4], and engineered phase matching giving rise to a second-harmonic beam with an Airy structure, which accelerates after emerging from a quadratic crystal [5]. This raises an intriguing question, Can self-accelerating solitons exist?

Optical spatial solitons have been studied for decades [6]. However, in almost all cases self-trapped beams propagate without bending their trajectories [7]. The core reason is the conservation of momentum. Exceptions occur when the nonlinearities are asymmetric—acting as an external force; hence, momentum is not conserved. For example, photorefractive solitons exhibit self-bending due to a small asymmetric contribution from the diffusion field [8], which is pronounced when an Airy beam is launched into an unbiased photorefractive crystal [9]. Another example occurs for temporal solitons in fibers, where the Raman effect adds an intensity-gradient term, causing acceleration [10]. Asymmetric response can also arise from asymmetric boundary conditions in nonlocal nonlinearities [11]. But, when the nonlinearity has no prescribed asymmetry and momentum is conserved, such as in Kerr or quadratic media, can a self-trapped beam self-accelerate? Attempts of launching an Airy beam into symmetric nonlinearities have shown that the beam shape varies, no longer propagating as accelerating self-trapped entity [12].

In 1979, temporal self-accelerating solitons were found in Kerr media [13], represented by the integrable cubic Schrödinger equation. This solution, which accelerates at a parabolic trajectory, is associated with the “second Painlevé transcendent.” This pioneering work raises many new intriguing questions. First, is integrability a necessary condition for accelerating self-trapped beams? To date, the majority of optical spatial solitons occur in nonintegrable systems. Can self-accelerating solitons occur in saturable or quadratic media? What nonlinearities can

support accelerating self-trapped beams? Second, the solution in [13] requires infinite power, unlike bright solitons which carry finite power (are square integrable). Do all accelerating self-trapped beams carry infinite power? Third, the trajectory in [13] is parabolic. What other trajectories are possible? Finally, how do accelerating self-trapped beams differ from their linear counterparts?

Here, we show that classes of symmetric nonlinearities can give rise to optical self-accelerating self-trapped beams. We demonstrate that Kerr, saturable Kerr-like, and quadratic media, which are the most common nonlinearities for generating spatial solitons, support self-accelerating self-trapped states. We prove that such solutions exist for any nonlinearity having a general intensity dependence $\Delta n = \Delta n(I)$, and that all accelerating beams have a parabolic trajectory. Finally, we investigate the properties of these nonlinear waves and compare them with linear Airy beams.

We start from the nonlinear paraxial equation in (1 + 1) dimensions for the slowly varying envelope:

$$i\psi_z + \frac{1}{2k}\psi_{xx} + \frac{k\Delta n}{n_0}\psi = 0. \quad (1)$$

where z is the optical axis, x is the transverse dimension, k is the wave number, n_0 is the linear refractive index, and Δn is the small real nonlinear change in the refractive index, which is a local function of $|\psi|^2$ [i.e., $\Delta n(x, z)$ is a function of $|\psi|^2$ at the same x, z]. The same derivation can include two transverse dimensions. We seek shape-preserving accelerating beams: stationary solutions in the accelerated frame. Such beams satisfy $|\psi(x, 0)| = |\psi(x - f(z), z)|$, meaning that the beam propagates along the curve $x = f(z)$ while maintaining its shape in x . In the linear case, the only possible curve an accelerating beam can take is parabolic [1]. Setting $\hat{x} = x - f(z)$ and changing the frame of reference to an accelerated one, yields

$$i\psi_z - if'(z)\psi_{\hat{x}} + \frac{1}{2k}\psi_{\hat{x}\hat{x}} + \frac{k\Delta n}{n_0}\psi = 0. \quad (2)$$

Any stationary solution in the accelerated frame is an accelerating self-trapped solution of the lab frame. We

seek solutions of the form $\psi(\hat{x}, z) = u(\hat{x})e^{i\theta(\hat{x}, z)}$. Seeking localized solutions, the imaginary part of (2) yields $f'' = c$, where c is a real constant. Hence, the trajectory must be parabolic, and the phase must be as in [1], giving $\theta(\hat{x}, z) = ck\hat{x}z + c^2kz^3/6$. Substituting this into (2) leads to

$$\frac{1}{2k}u'' + \frac{k\Delta n}{n_0}u - (\hat{x} - \hat{x}_0)cku = 0. \quad (3)$$

In the linear case, Eq. (3) is solved by the Airy function. Therefore, we expect the solution for a weak nonlinearity (or for a small amplitude) to be similar to the Airy beam.

Thus far, we showed that even outside the linear regime, the only allowed trajectory of a self-accelerating beam is parabolic. Moreover, any nonlinearity which is homogeneous in space and involves no imaginary part can support only shape-preserving accelerating solutions with a parabolic trajectory. We first study systems exhibiting Kerr and Kerr-like saturable nonlinearities, and subsequently explore the fundamentally different case of quadratic media.

Domains of stationary solutions.—Substituting the Kerr nonlinearity $\Delta n = n_2u^2$ in (3) and transforming to dimensionless coordinates [14] yields

$$U'' + 2 \operatorname{sgn}(n_2)U^3 - XU = 0, \quad (4)$$

where $x - x_0 = X/\sqrt[3]{2ck^2}$ and $u = U\sqrt[3]{2c/k}/\sqrt{|n_2/n_0|}$. The nonlinear term is of the focusing (defocusing) type for $n_2 > 0$ ($n_2 < 0$). We solve (4) numerically by noting that for $X \rightarrow \infty$ the amplitude is small enough such that the nonlinear term is negligible. Hence, we use the Airy solution of the linear equation to set the boundary conditions at large X , and integrate (4) from there on. The linear solution $U = \alpha \operatorname{Ai}(X)$ has α as a trivial degree of freedom. In the nonlinear domain α gives a family of nontrivial solutions, forming a 1D solutions space, where the free parameter is the nonlinearity strength. The solutions space is separated [13] into focusing, where localized solutions exist for any $n_2\alpha^2 > 0$, and defocusing, where localized solutions exist only for $-1 < n_2\alpha^2 < 0$. These domains merge as $n_2\alpha^2 \rightarrow 0$. See Fig. 1 for examples.

Asymptotic behavior.—All accelerating solutions have the same Airy-like tail for $X \rightarrow -\infty$ [Fig. 1, top row], because U tends to zero as $X \rightarrow -\infty$, so the nonlinear term tends to zero. Hence, the solutions asymptotically coincide with the Airy function. This phenomenon occurs for any solution which asymptotically tends to zero, in any local nonlinearity. The beams' tails are not identical to the Airy tail: they match only asymptotically. Indeed, launching the linear (Airy) solution into nonlinear media alters the beam structure [12]: the sidelobes become asynchronous as the propagation velocities depend on the local index, which in turn depends on the local amplitude. Consequently, when such a beam emerges from the nonlinear medium, it no longer exhibits acceleration [12]. Instead, one should launch the specific wave function to initiate stationary propagation in the accelerating frame.

Stability.—We study the stability of the nonlinear self-accelerating beams numerically, under Gaussian white

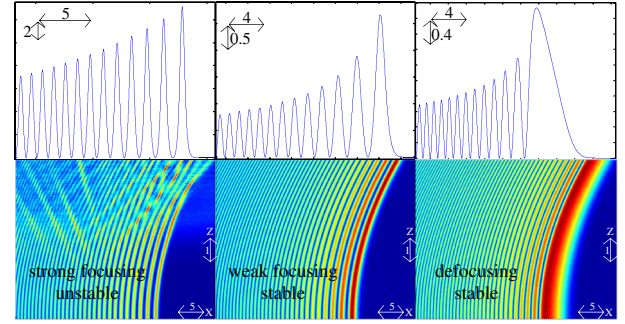


FIG. 1 (color online). Self-accelerating beams in Kerr media. Top row: Intensity profiles at $z = 0$. Bottom row: Propagation of self-accelerating beams with infinite tails and 2% noise. Left column: Strong focusing nonlinearity. Middle column: Weak focusing nonlinearity. Right column: Defocusing nonlinearity.

noise. Examples are shown in Fig. 1. We find that accelerating beams under defocusing conditions propagate in a stable fashion (Fig. 1, bottom right). Second, accelerating beams under weak self-focusing are also stable (Fig. 1, bottom center). However, accelerating beams under strong self-focusing are unstable: the strong lobes of the beam form solitons, which are emitted in various directions (Fig. 1, bottom left). Surprisingly, the first lobe of such a beam continues accelerating even after emitting solitons. The transition from stability to instability can be explained qualitatively: the instability always begins at the first lobe, which breaks into filaments, emitted as stand-alone solitons. The question is under what conditions the first lobe becomes unstable. The answer relies on the knowledge of solitons: any localized beam of width more than twice the width of a soliton of the same intensity tends to break up into two (or more) solitons [15]. When this first lobe is narrower than twice the width of the associated soliton, the beam is propagating as a self-trapped entity (with some breathing) for large distances. We find numerically that this logic applies also to our accelerating self-trapped beams, where the stability of the whole beam is determined by the stability of the first lobe. We therefore find the transition from stability to instability by plotting the existence curve of the first lobe, and check when it crosses the curve of a beam with twice the width of a soliton of the same intensity [Fig. 2(a), dashed line crossing the bottom line]. This black line separates the existence curve of the focusing nonlinearity to the stable region (on the left) and unstable region (on the right). The stability of the accelerating self-trapped beams has an additional aspect: far enough from the first lobe, the beam is weaker than the noise. This issue is addressed in the section on finite-power beams.

Extreme self-focusing and self-defocusing.—Next, we examine the case of extreme self-focusing. This solution (Fig. 1, left column) differs significantly from the Airy beam: the main lobe is no longer much wider than the subsequent lobes (compare to Fig. 1, middle column); rather, it is almost an exact enlarged replica of the second lobe. For extreme self-focusing the lobes are almost fully

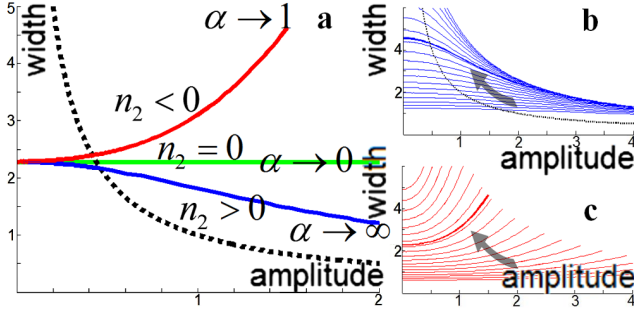


FIG. 2 (color online). (a) Existence curves of the self-accelerating beams. (b),(c) Existence curves when varying the acceleration; normalized acceleration in bold. Arrow points to the direction of higher acceleration. Nonlinearity type: focusing (bottom line), defocusing (top line), linear (middle line). The broken line describes the existence curve for a Kerr soliton.

self-similar, differing only in size. The other extreme nonlinear case occurs for $n_2 < 0$, exhibiting a threshold for the existence of a stationary localized beam. Above this threshold, the intensity is too high, and defocusing is too strong to be balanced by acceleration. The right column in Fig. 1 presents the accelerating beam with nonlinearity very close to the threshold. The nonlinearity makes the first lobe much wider than the linear Airy beam.

Role of acceleration.—Figure 2(a) displays the existence curve of the accelerating self-trapped beams, showing width of the first lobe versus its amplitude. Each accelerating solution is a point on the curve. The existence curve also explains the acceleration. Varying the acceleration parameter in the units' transformation while keeping the other parameters constant yields the existence curves for focusing and defocusing [Figs. 2(b) and 2(c), respectively], displaying width versus amplitude for the first lobe. Different curves represent different accelerations, displaying a limiting behavior for both high and small accelerations. For example, in Fig. 2(b) the curves on the right tend to a convex curve of (almost) zero acceleration, whereas the curves on the left tend to a steep curve of large intensity. Near this steep curve, even a small change in width greatly increases the acceleration. It is unclear if there is a limit or the curves cover the whole phase space. If there is a limit curve, it has interesting implications, such as a minimum width for any nonlinear self-accelerating beam. Figures 2(b) and 2(c) reveal that larger acceleration implies narrower lobes in either focusing, defocusing, or without nonlinearity. Higher intensity yields smaller acceleration in focusing media and larger acceleration in defocusing media.

Structure of accelerating solution.—Summarizing the parametric study of the accelerating self-trapped beams from their existence curves, we point out several results [14]. First, defocusing is better for channeling a larger fraction of power in the accelerating main lobe, because the main lobe is wider under strong defocusing but narrower with strong focusing. Second, focusing supports two kinds of accelerating structures: in the stable weakly nonlinear regime the beam is Airy-like, whereas in the

unstable strongly nonlinear regime the beam has a “porcupine” structure, with increasingly narrower lobes of lower amplitude. Interestingly, the “needlelike” shape of the lobes is self-similar: all have the same shape, yet their width scales with their decreasing amplitude. The transition between the two regimes occurs at the same point where the existence curves of the accelerating beam and of the soliton associated with the first lobe cross each other [Fig. 2(a); see also [14], Sec. 4].

Self-accelerating beams carrying finite power.—All stationary solutions of the accelerated equation with $\Delta n = \Delta n(|\psi|^2)$ carry infinite power, because their tails coincide with the Airy function which is not square integrable. Launching truncated beams acts similar to the linear case [2]: the beams accelerate for a finite distance only, which depends on the aperture and the acceleration. This behavior is similar to what happens when noise is superimposed on a beam of infinite extent: far enough from the first lobe, the noise is stronger than the beam amplitude, causing the same effects as if the beam were truncated at that point [14].

Self-accelerating beams in saturable nonlinearities.—Saturable media also support accelerating beams. Their derivation follows the lines of Eq. (3), and they are found in the same fashion. Some of their properties are similar to those in Kerr media, while some features are different [14].

Self-accelerating beams in quadratic media.—This case involves two coupled waves $\psi^{(1)}, \psi^{(2)}$ (first and second harmonics). This system is far from the nonlinearities represented by Eqs. (1)–(4), and the nonlinear terms are complex, allowing power exchange between the waves. The coupled equations, under perfect phase matching, are

$$\begin{aligned} i\psi_z^{(1)} + \frac{1}{2k}\psi_{xx}^{(1)} + k\beta_1\psi^{(2)}(\psi^{(1)})^* &= 0, \\ i\psi_z^{(2)} + \frac{1}{4k}\psi_{xx}^{(2)} + 2k\beta_2(\psi^{(1)})^2 &= 0. \end{aligned} \quad (5)$$

Transforming variables yields two coupled equations. Since (5) is not a particular case of (2), and the nonlinearity is not real valued, the restrictions forcing a parabolic curve for the solutions of Eq. (3) do not hold here; hence, stationary solutions with nonparabolic curves may also exist. However, using a parabolic curve simplifies Eq. (5), giving coupled equations for the normalized amplitudes U_1, U_2 :

$$U_1'' + 2U_1U_2 - XU_1 = 0, \quad U_2''/4 + 2U_1^2 - XU_2 = 0, \quad (6)$$

with the normalization $\hat{x} = X(2k^2c)^{-1/3}$, $u^{(2)} = U_2(2c/k)^{2/3}/\beta_1$, $u^{(1)} = U_1(2c/k)^{2/3}/\sqrt{\beta_1\beta_2}$.

Let us first require $U_2(X \rightarrow \infty) \rightarrow 0$. Hence, for large enough X we can approximate the first equation by its linear version, with a localized solution $U_1 = \alpha_1 \text{Ai}(X)$. Under this approximation, the second equation becomes also linear but has an inhomogeneous part, yielding $U_2 = \alpha_2 \text{Ai}(2^{2/3}X) + \alpha_1^2 F(X)$ with $F(X)$ being its particular solution (which can be found explicitly). Consequently, the family of solutions is 2D (controlled by two amplitudes α_1, α_2) [5], and is divided roughly into two domains: (I) $\alpha_1^2 > \alpha_2$, where the Airy function is the dominant part

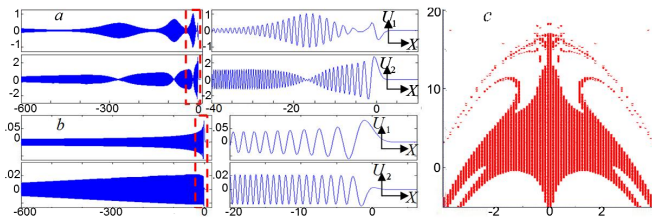


FIG. 3 (color online). Self-accelerating beams in quadratic media. Amplitude profiles for $\alpha_1 = \alpha_2 = -3.8$ (a) and $\alpha_1 = 0.15, \alpha_2 = 0$ (b). (a),(b) Top (bottom) row: Amplitude of the first (second) harmonic wave. Left column: Wide view of the beams showing many lobes of the infinite tail. Right column: Close-up of the marked regions, showing the lobes adjacent to the main lobe. (c) Existence domain of accelerating solutions with the axes α_1 (horizontal) and α_2 (vertical).

of the two-frequency wave, and (II) $\alpha_1^2 < \alpha_2$, which exhibits a non-Airy-type solution. When α_1, α_2 are large enough, the Airy waves interfere asynchronously; yet surprisingly there is still a localized solution. An example is given in Fig. 3(a), showing asynchronously coupled first- and second-harmonic beams, accelerating along the *same* parabolic trajectory. The right column shows U_1, U_2 near the main lobe, exhibiting shapes differing significantly from any known accelerating beam. The left column shows U_1, U_2 with a long tail, highlighting the power exchange between the beams. Two frequencies dominate each beam: the basic lobes frequency and a slower envelope frequency. The frequency of the lobes grows as $X \rightarrow -\infty$, while the envelope frequency gets smaller as X gets smaller. This is expected since, for a smaller X , the amplitude gets smaller and the nonlinear coupling gradually disappears, matching two independent Airy beams. We expect additional phenomena at different parameters regimes, but the two-frequency asynchrony remains; see, e.g., Fig. 3(b). The existence domain is plotted in Fig. 3(c) [14]. We test the stability of accelerating self-trapped beams in quadratic media by simulating Eq. (5) using standard beam propagation methods. We find that the solutions of Figs. 3(a) and 3(b) are both numerically stable, even in the presence of noise at the level of 1% of the maximum intensity, distributed uniformly in the transverse plane.

Experimental observables.—Accelerating nonlinear beams are experimentally accessible. For example, consider a beam of 500 nm wavelength, going through an 0.8 mm aperture within which its structure is shaped to launch an accelerating beam in Kerr media. The aperture allows 80 lobes with widths varying from 30 μm (main lobe) to 10 μm (farthest lobe). The intensity is such that the maximum index change is 0.5×10^{-5} (at the peak of the main lobe), which is readily accessible in semiconductors. After propagating 5 cm, the main lobe moves laterally 0.5 mm. The acceleration stops after 6 cm, due to the finite aperture. This beam exhibits many of the phenomena described above, e.g., the self-similar porcupine shape

and the associated emitted solitons under strong self-focusing.

In conclusion, we proposed shape-preserving accelerating beams in nonlinear media that propagate along parabolic trajectories and derived their existence curve. We discussed other self-accelerating beams, especially the asynchronous solutions for quadratic nonlinearities. We studied finite aperture effects and showed how accelerating beams can be implemented experimentally. Applications are expected for high intensity beams, where the acceleration can be changed by varying the intensity. Other applications arise for nonlinear accelerating beams in media displaying thermophoresis or photophoresis [16], where light controls the local density of particles within the liquid or gas [16]. Another application relates to Airy beams that accelerate both in space and in time [17,18]. The experiment in [18] reports an upper limit on the optical intensity enforced by “the nonlinearly induced distortions.” With the concept introduced here, the nonlinearity is no longer a distortion: it makes it possible to launch an accelerating light bullet, self-trapped in both space and time.

This work was supported by an Advanced Grant from the ERC.

-
- [1] M. V. Berry and N. L. Balazs, *Am. J. Phys.* **47**, 264 (1979).
 - [2] G. A. Siviloglou and D. N. Christodoulides, *Opt. Lett.* **32**, 979 (2007); G. A. Siviloglou *et al.*, *Phys. Rev. Lett.* **99**, 213901 (2007).
 - [3] J. Baumgartl *et al.*, *Nat. Photon.* **2**, 675 (2008).
 - [4] P. Polynkin *et al.*, *Science* **324**, 229 (2009).
 - [5] T. Ellenbogen *et al.*, *Nat. Photon.* **3**, 395 (2009).
 - [6] G. I. Stegeman and M. Segev, *Science* **286**, 1518 (1999).
 - [7] Notwithstanding high-order solitons, which display oscillatory propagation, but not self-acceleration.
 - [8] M.-f. Shih *et al.*, *Opt. Lett.* **21**, 324 (1996); M. Segev *et al.*, *Phys. Rev. Lett.* **73**, 3211 (1994); D. N. Christodoulides *et al.*, *J. Opt. Soc. Am. B* **12**, 1628 (1995).
 - [9] D. N. Christodoulides *et al.*, *Opt. Lett.* **21**, 1460 (1996); S. Jia *et al.*, *Phys. Rev. Lett.* **104**, 253904 (2010).
 - [10] A. V. Gorbach and D. V. Skryabin, *Phys. Rev. A* **76**, 053803 (2007).
 - [11] B. Alfassi *et al.*, *Opt. Lett.* **32**, 154 (2007).
 - [12] Y. Hu *et al.*, *Opt. Lett.* **35**, 3952 (2010); R.-P. Chen *et al.*, *Phys. Rev. A* **82**, 043832 (2010).
 - [13] J. A. Giannini and R. I. Joseph, *Phys. Lett. A* **141**, 417 (1989).
 - [14] See supplemental material at <http://link.aps.org/supplemental/10.1103/PhysRevLett.106.213903> for details and examples.
 - [15] S. Sears *et al.*, *Phys. Rev. Lett.* **84**, 1902 (2000).
 - [16] Y. Lamhot *et al.*, *Phys. Rev. Lett.* **105**, 163906 (2010); V. G. Shvedov *et al.*, *ibid.* **105**, 118103 (2010).
 - [17] A. Chong *et al.*, *Nat. Photon.* **4**, 103 (2010).
 - [18] D. Abdollahpour *et al.*, *Phys. Rev. Lett.* **105**, 253901 (2010).